

## **Chapter 6. Neutral droplets in high electric fields as a source of ions. Introduction to field-induced droplet ionization mass spectrometry**

Adapted from Grimm, R. L. and Beauchamp, J. L. *J. Phys. Chem. B.* **2003**, *107*, 14161.

### **6.1. Abstract**

A neutral droplet elongates along the axis of a strong electric field, ejecting opposing jets of positively and negatively charged progeny droplets. Images of droplets from a vibrating orifice aerosol generator illustrate this phenomenon, and mass spectrometric sampling of the progeny droplets demonstrates that they are a viable source of desolvated gas-phase ions. Field induced droplet ionization (FIDI) mass spectra are presented for several species, including tetraheptylammonium cation, deprotonated benzene tetracarboxylic acid anion, and multiply protonated cytochrome *c*.

### **6.2. Letter**

We report a method for generating desolvated ions in the gas phase, based on neutral droplet instability in strong electric fields. This experimental methodology facilitates new applications of mass spectrometry to problems in chemistry and biology. In a sufficiently high electric field, neutral droplets elongate parallel to the field, developing two opposing conical tips that emit fine jets. These jets break up into droplets that we assume are charged opposite of the electrode to which they are attracted. We

demonstrate that the progeny droplets formed by field-induced droplet ionization (FIDI) comprise a viable source of ions for mass spectrometric analysis.

Early explorations into the effect of electric fields on water droplets and soap films led to eq (6.1) for the electric field  $E$  necessary to induce an instability leading to a discharge event in a drop or film of radius  $r$ .<sup>1-5</sup> In eq (6.1),  $\sigma$  is the surface tension of the liquid,  $\epsilon_0$  is the permittivity of free space, and  $c$  is an experimentally determined parameter. Seminal theoretical work on droplets in electric fields is due to Taylor.<sup>5,6</sup> His leaky dielectric model predicts that droplets elongate into prolate ellipsoids, axisymmetric with the applied electric field. At a critical electric field referred to as the Taylor limit, the prolate shape becomes unstable leading to the formation of fine jets.

$$E^2 = c \frac{\sigma}{4\pi\epsilon_0 r} \quad (6.1)$$

Elaborating the simplified analysis that led to eq (6.1) and theoretically modeling droplet deformation and breakup phenomena is still an active field of research in fluid dynamics.<sup>7-11</sup> Experimental investigations of suspended droplets are in general agreement with Taylor's theoretical predictions.<sup>12,13</sup> Small experimental deviations from theory are evident in the independent investigations due to Nolan<sup>3</sup> and Macky<sup>4</sup> of water droplets passing through an electric field. Both observed discharge events occurring at electric field strengths somewhat lower than predicted theoretically. Taylor suggested aerodynamic effects might have been responsible for the discrepancies<sup>5</sup> since the droplets were falling in air. With theoretical and experimental investigations focused on parent droplets and their instability in strong electric fields, the properties of progeny droplets formed in the process have been largely ignored.

In the present study, we demonstrate that progeny droplets are a viable source of both positively and negatively charged gas-phase ions for mass spectrometric analysis. Droplets are imaged using a pulsed xenon flashlamp in combination with a high-resolution CCD camera while the emitted jets are characterized using mass spectrometry. Figure 6.1 shows a schematic of the experimental arrangement. We chose methanol because equation (6.1) suggests its lower surface tension ( $0.022 \text{ N m}^{-1}$  versus  $0.072 \text{ N m}^{-1}$  for water) requires lower electric fields to reach the Taylor limit. A vibrating orifice aerosol generator (VOAG) generates  $\sim 170 \text{ }\mu\text{m}$  diameter methanol droplets at  $17.3 \text{ kHz}$ . Droplets pass between two parallel plate electrodes spaced  $1.4 \text{ mm}$  apart that define the electric field. The left hand electrode is electrically grounded while the right hand electrode is held at high voltage. The xenon flashlamp is synchronized with the VOAG to illuminate the droplets at fixed positions.

Figure 6.2 shows the deformation of a methanol droplet with jet formation in a  $2.2 \times 10^6 \text{ V m}^{-1}$  electric field. This is similar to the  $2.3 \times 10^6 \text{ V m}^{-1}$  field suggested from Macky's analysis<sup>4</sup> but lower than the  $2.5 \times 10^6 \text{ V m}^{-1}$  field calculated from Taylor's theory<sup>5</sup> when applied to  $170 \text{ }\mu\text{m}$  methanol droplets. We do not explain this difference except to note that our experiment is conducted on moving droplets similar to Nolan<sup>3</sup> and Macky.<sup>4</sup> The field stretches the droplets into prolate ellipsoids with two opposing conical tips ejecting oppositely charged jets of methanol progeny droplets. This is visually similar to the symmetrical Rayleigh discharge process observed by Leisner and coworkers for ethylene glycol droplets,<sup>14</sup> although that event results in the ejection of

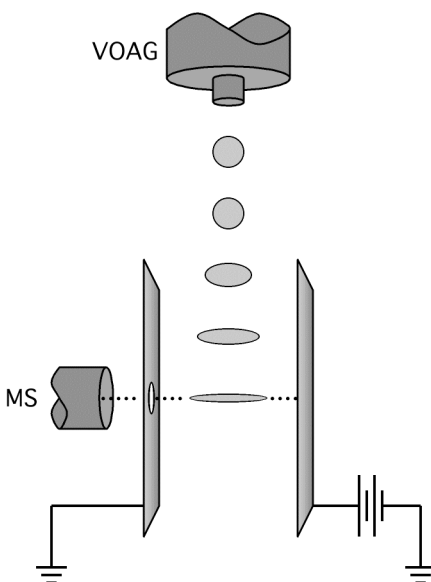


Figure 6.1. Experimental arrangement for FIDI-MS. A vibrating orifice aerosol generator (VOAG) produces droplets that pass through an electric field defined by two parallel plate electrodes. The electrode on the left is held at ground while the one on the right is held at high voltage. Droplets elongate and symmetrically emit two oppositely charged jets towards the electrodes. The jet directed at the left hand plate passes through an aperture to be sampled by a mass spectrometer (MS).

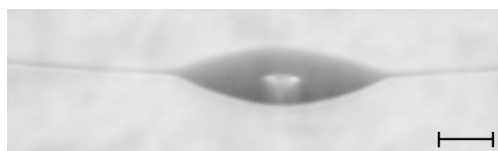


Figure 6.2. Image of a single 170  $\mu\text{m}$  diameter methanol droplet illustrating jets formed at conical tips with a field strength of  $2.2 \times 10^6 \text{ V m}^{-1}$ . The droplet, moving downward in the figure, is illuminated by a single pulse from a xenon flashlamp and imaged through a microscope onto a high-resolution CCD camera. Aerodynamic drag is responsible for the slight upward curvature of the two progeny jets. The bar indicates 100 microns.

similarly charged jets from a parent droplet with an overall net charge. This contrasts with unsymmetrical Rayleigh discharge events observed for droplets charged by a corona discharge<sup>15,16</sup> or electrospray ionization<sup>17</sup> in high electric fields.

Mass spectrometry supports the conjecture of the formation of oppositely charged jets. An aperture within one plate allows an aligned desolvation capillary inlet of a mass spectrometer (Figure 6.1) to sample the progeny droplets. In principle, a pair of mass spectrometers may simultaneously sample the positive and negative progeny droplets. In the single mass spectrometer configuration, positive ions are sampled using positive high voltage on the right hand plate. Similarly, the mass spectrometer samples negative progeny when the right hand plate is held at negative high voltage. A Finnigan LCQ Classic ion trap mass spectrometer with a custom-built desolvation capillary extension is employed for mass analysis.

To demonstrate that both positive and negative ions may be sampled from the same droplet, we tested a combined solution of 100  $\mu\text{M}$  tetraheptylammonium bromide (THAB) and 100  $\mu\text{M}$  1,2,4,5 benzene tetracarboxylic acid (BTCA) in methanol under identical VOAG conditions and identical but reversed electric fields for both positive and negative ions. In positive ion mode (Figure 6.3a), the mixed THAB/BTCA solution mass spectrum exhibits the tetraheptylammonium ion peak at 410  $m/z$  and the bromide-bound tetraheptylammonium dimer at 900  $m/z$ . In negative ion mode (Figure 6.3b), we observe a peak at 253  $m/z$  indicative of singly deprotonated BTCA, and a peak at 662  $m/z$  attributed to a doubly deprotonated BTCA anion complexed to a tetraheptylammonium cation. Each spectrum is consistent with mass spectra acquired for this solution with a

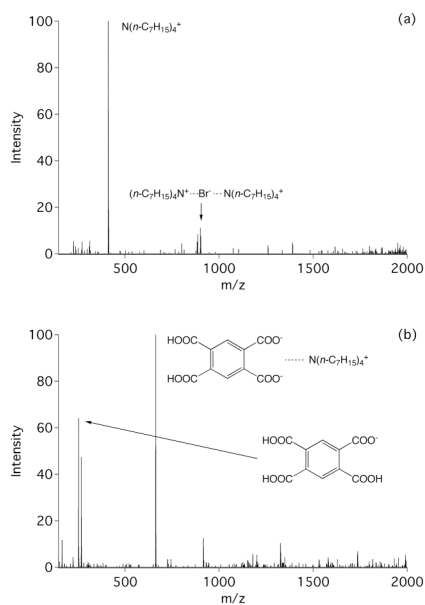


Figure 6.3. Positive ion (a) and negative ion (b) mass spectra of a solution of 100  $\mu$ M THAB and 100  $\mu$ M 1,2,4,5 BTCA. The positive ion spectrum consists of the tetraheptylammonium ion at 410 m/z and the bromide-bound tetraheptylammonium dimer at 900 m/z. The singly deprotonated BTCA species at 253 m/z and a doubly deprotonated BTCA - tetraheptylammonium cation adduct at 662 m/z dominate the negative ion mass spectrum.

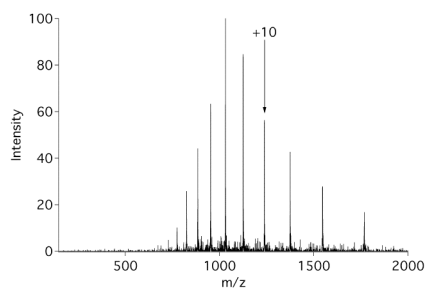


Figure 6.4. Horse heart cytochrome *c* mass spectrum of a 20  $\mu$ M solution in 80% methanol, 20% water, and 0.1% acetic acid. The broad distribution of charge states acquired with the FIDI-MS technique closely resembles the positive-mode ESI mass spectrum of the same solution.

conventional electrospray ionization (ESI) source, including the expected isotopic distributions. We additionally tested a 20  $\mu$ M solution of horse heart cytochrome *c* in 80% methanol, 20% water, and 0.1% acetic acid (Figure 6.4). The peak distribution in Figure 6.4 resembles that observed in an ESI mass spectrum of the same solution.

Droplet discharge events induced by strong electric fields are a route to charged progeny droplets and gas phase ions through a process we call field induced droplet ionization, or FIDI. Other methods used to sample ionic components of neutral droplets include injecting them into a corona discharge, where they become highly charged,<sup>16</sup> or allowing them to fuse with highly charged droplets formed by electrospray.<sup>18</sup> In both instances, subsequent events leading to desolvated ions are the same as in ESI. The mass spectra from FIDI-MS resemble ESI mass spectra. However, the possibility of simultaneously extracting both positive and negative ions from a neutral droplet, without the constraint of the capillary needle required for ESI-MS, opens avenues in chemical and biological research unavailable with current techniques. For example, environmental studies involving the real-time analysis of liquid aerosols can benefit from the simultaneous sampling of both positively and negatively charged species from the same droplet. Variations may involve the analysis of a single droplet, repeated sampling of an individual droplet, or the use of pulsed electric fields to analyze specifically selected droplets. Ongoing investigations in our lab are exploring the parameter space related to FIDI, with the goal of quantifying the role of droplet size, charge carriers and their mobility, and bulk solvent characteristics such as dielectric constant and viscosity. The ultimate sensitivity of the method will depend on the development of an optimized interface for efficient ion transfer to the mass spectrometer.

### **6.3. Acknowledgements**

The authors gratefully acknowledge Drs. Nathan Dalleska and Mona Shahgholi for the assistance with and use of their mass spectrometry facilities. The Beckman Institute at Caltech has provided facilities and financial support for these investigations. Studies of droplet evaporation and discharge processes associated with ESI have been supported by National Science Foundation grant CHE-9727566.



## 6.4. References

- (1) Zeleny, J. *Phys. Rev.* **1917**, *10*, 1.
- (2) Wilson, C. T. R.; Taylor, G. I. *Proc. Cambridge Philos. Soc.* **1925**, *22*, 728.
- (3) Nolan, J. J. *Proc. R. Ir. Acad. Sect. A* **1926**, *37*, 28.
- (4) Macky, W. A. *Proc. Roy. Soc. A* **1931**, *133*, 565.
- (5) Taylor, G. *Proc. R. Soc. London, Ser. A* **1964**, *280*, 383.
- (6) Taylor, G. *Proc. R. Soc. London, Ser. A* **1966**, *291*, 159.
- (7) Miksis, M. J. *Phys. Fluids* **1981**, *24*, 1967.
- (8) Basaran, O. A.; Scriven, L. E. *Phys. Fluids A* **1989**, *1*, 799.
- (9) Basaran, O. A.; Patzek, T. W.; Benner, R. E.; Scriven, L. E. *Ind. Eng. Chem. Res.* **1995**, *34*, 3454.
- (10) Stone, H. A.; Lister, J. R.; Brenner, M. P. *Proc. R. Soc. London, Ser. A* **1999**, *455*, 329.
- (11) Zholkovskij, E. K.; Masliyah, J. H.; Czarnecki, J. *J. Fluid Mech.* **2002**, *472*, 1.
- (12) Vizika, O.; Saville, D. A. *J. Fluid Mech.* **1992**, *239*, 1.
- (13) Eow, J. S.; Ghadiri, M. *Chem. Eng. Process.* **2003**, *42*, 259.
- (14) Duft, D.; Atchtzehn, T.; Muller, R.; Huber, B. A.; Leisner, T. *Nature* **2003**, *421*, 6919.
- (15) Hager, D. B.; Dovichi, N. J. *Anal. Chem.* **1994**, *66*, 1593.
- (16) Hager, D. B.; Dovichi, N. J.; Klassen, J.; Kebarle, P. *Anal. Chem.* **1994**, *66*, 3944.
- (17) Gomez, A.; Tang, K. *Phys. Fluids* **1994**, *6*, 404.
- (18) Chang, D.-Y.; Lee, C.-C.; Shiea, J. *Anal. Chem.* **2002**, *74*, 2465.

